UNITED STATES POSTAL SERVICE

ADVANCED TECHNOLOGY CONFERENCE

MAY 3—5, 1988

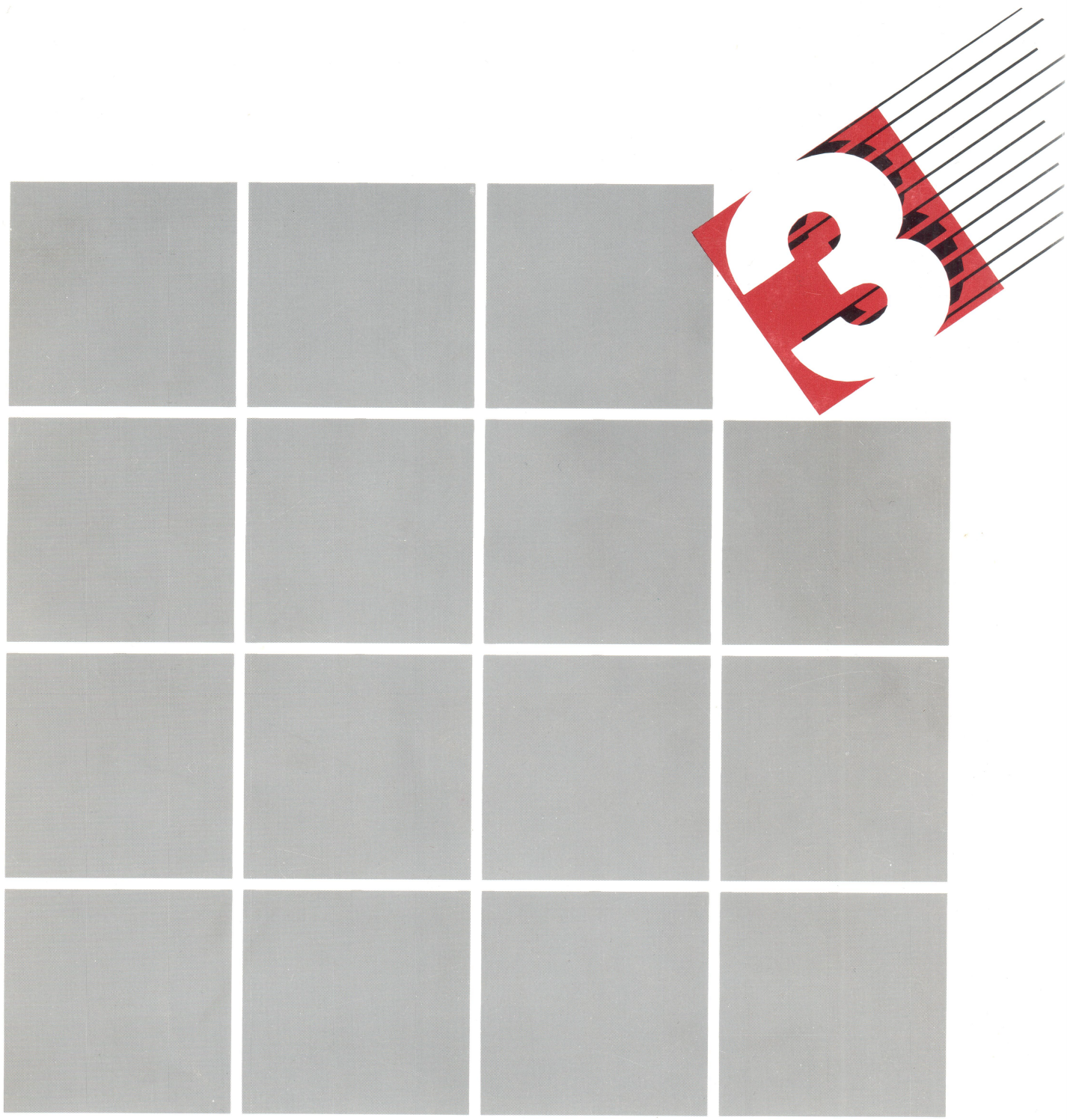

VOLUME TWO

CONFERENCE COMMITTEE

General Chairman

Gary P. Herring
Director
Office of Advanced Technology

Program Co-Chairmen

Timothy B. Barnum, Ph.D.
Program Director
Office of Advanced Technology

Frederick R. Glickman, Ph.D.
Program Director
Office of Advanced Technology

Keynote Technology Speakers

Alvin M. Despain, Professor
University of California, Berkeley

Robert Hecht-Nielsen, Ph.D.
Chair of Board
Hecht-Nielsen Neurocomputers Corporation

Lotfi Zadeh, Professor
University of California, Berkeley

Session Chairmen

Ruzena Bajcsy
Timothy B. Barnum
Warren P. Denise
Alvin M. Despain
Fred J. DiLisio
Frederick R. Glickman
Robert Hecht-Nielsen
Avi C. Kak
Samuel J. Mehlman
Prasanna G. Mulganokar
David Nitzan
Sargur N. Srihari

Conference Coordinator

Linda J. Mahoney

Secretary

Evelena C. Carroll

SHAPE RECOVERY OF MAIL PIECES USING DEFORMABLE MODELS

Franc Solina and Ruzena Bajcsy
Department of Computer and Information Science
University of Pennsylvania, Philadelphia PA

ABSTRACT

A system for classification of mail pieces using range images is proposed. Position, orientation, size and shape parameters of volumetric models of single mail pieces are recovered using least squares minimization of a fitting function. The models are superquadrics with global deformations. The recovered parameters serve for classification.

I. INTRODUCTION

Automatic sorting of all mail pieces is a difficult problem because mail pieces differ widely in size and shape. In general, one has to know the location, orientation, size and shape of mail pieces to be able to initiate the right handling procedure. Computer vision as a method for locating and describing of objects without direct physical contact seems to be the right approach to do that in a fast and reliable manner.

Computer vision has been successfully applied in many industrial applications. The methods used in the majority of these industrial vision systems, however, cannot be applied to the problem of mail piece classification. Most so called "model-based" object recognition vision systems use a set of rigid and precise models for all objects that are expected to be found in the scene [1]. Based on detected local features in the scene, these models are projected onto the image, to find if they match with the rest of the image features. This approach is possible only in tightly controlled environments where the shape of objects is well defined and the number of different objects is small. This is clearly not the case with mail pieces, which come in a variety of sizes and shapes.

When precise object models are not available, traditional computer vision advocates a stepwise reduction of data [2]. First, low level shape models such as edges, corners and surface patches are computed locally. Due to the small granularity of these models, a large number of such models is required even for simple scenes. To do any reasoning about the scene, these local models must be merged into larger entities, generalized cylinders being the most popular. In the case of mail pieces, this merging of local models is difficult and error-prone because mail pieces do not conform to perfect

geometrical shapes due to rounded edges, distorted corners, bulging sides and wrinkled surfaces. We believe that such bottom-up approach would not be successful for classifying mail pieces from range images.

At the second USPS Advanced Technology conference we proposed to use volumetric models of larger granularity - superquadric models with deformations - to interpret mail pieces [3]. Additional information which is needed for patching up the missing information and rejecting the erroneous local information can be supplied by compact volumetric models if they have the right granularity. One superquadric model is in general sufficient for modeling of a single mail piece. The parameters of these superquadric models can be recovered directly from range images. The recovery can be explained in terms of intrinsic and extrinsic forces. Intrinsic forces are the internal properties of the model, governing its potential shape, while the extrinsic forces govern the possible arrangement of internal properties. Since superquadrics can model most common geometrical shapes, such as parallelepipeds, cylinders, ellipses and shapes in between, they are appropriate to model most of the mail pieces. The initial proposal that we made in [3] has evolved over time [4, 5] and in this paper we report about the current implementation.

The rest of the paper is organized as follows: section II is a short introduction to superquadrics, section III describes model recovery, and section IV is on classification. Discussion in section V compares the advantages and deficiencies of the method and points to future extensions, especially to the use of such shape recovery for segmentation. We used range images from various sources, all of the range images in this paper, however, were obtained with a laser imager built at University of Pennsylvania [6]. Before model recovery, the supporting surface was removed by fitting a plane to it and subtracting the points on or close to that plane.

II. SUPERQUADRICS

Superquadrics are an extension of basic quadric surfaces and solids. Superquadrics have been used or proposed for use as primitives for shape representation in computer graphics [7] and computer vision [8]. Superquadrics can be compared to lumps of clay that can be further deformed and glued together into realistic looking models as is nicely demonstrated by Pentland's *Supersketch* graphics system [8].

Superquadrics are defined by the following equation

$$F(x, y, z) = \left[\left[\left[\frac{x}{a_1} \right]^{\frac{2}{\varepsilon_2}} + \left[\frac{y}{a_2} \right]^{\frac{2}{\varepsilon_2}} \right]^{\frac{\varepsilon_2}{\varepsilon_1}} + \left[\frac{z}{a_3} \right]^{\frac{2}{\varepsilon_1}} \right]^{\varepsilon_1}. \qquad (1)$$

When both ε_1 and ε_2 are 1, the surface vector defines an ellipsoid or, if a_1, a_2, a_3 are all equal, a sphere. When ε_1 is << 1 and $\varepsilon_2 = 1$, the superquadric surface is shaped like a cylinder (Figure 2). Parallelepipeds are produced when both ε_1 and ε_2 are << 1 (Figures 1 and 3). Modeling capabilities of superquadrics can be enhanced by deforming them in different ways, including tapering and bending (Figure 4).

The function in equation (1) is called the inside-outside function because it determines where a given point $[x, y, z]^T$ lies relative to the superquadric surface. If $F(x, y, z) = 1$, point (x, y, z) is on the surface of the superquadric. If $F(x, y, z) > 1$, the corresponding point lies outside and if $F(x, y, z) < 1$, the corresponding point lies inside the superquadric.

The inside-outside function (1) defines the superquadric surface in an object centered coordinate system (x_S, y_S, z_S). Input 3-D points from range images, on the other hand, are expressed in a world coordinate system. To express the inside-outside function for a superquadric in general position we use a homogeneous transformation **T**. The elements of the rotational part of transformation matrix **T** is expressed with Euler angles (ϕ, θ, ψ) [9]. The inside-outside function for superquadrics in general position is

$$F(x, y, z) = F(x, y, z; a_1, a_2, a_3, \varepsilon_1, \varepsilon_2, \phi, \theta, \psi, p_x, p_y, p_z). \tag{2}$$

This expanded inside-outside function has 11 parameters; a_1, a_2, a_3 define the superquadric size; ε_1 and ε_2 are for shape; ϕ, θ, ψ for orientation, and p_x, p_y, p_z for position in space. We refer to the set of all model parameters as $\Lambda = \{a_1, a_2, \cdots, a_{11}\}$.

III. RECOVERY OF SUPERQUADRIC MODELS

Suppose we have N 3-D surface points (x_W, y_W, z_W) which we want to model with a superquadric. We want to vary the 11 parameters a_j, $j = 1, \ldots, 11$ in equation (2) to get such values for a_j's that most of the 3-D points will lay on, or close to the model's surface. There will probably not exist a set of parameters Λ that perfectly fits the data. Finding the model Λ for which the distance from points to the model is minimal is a least-squares minimization problem. Since, for a point $[x_W, y_W, z_W]^T$ on the surface of a superquadric $F(x_W, y_W, z_W; a_1, \ldots, a_{11}) = 1$, we have to find

$$\min \sum_{i=1}^{N} [1 - F(x_{W_i}, y_{W_i}, z_{W_i}; a_1, \ldots, a_{11})]^2 . \tag{3}$$

Due to self occlusion, not all sides of an object are visible at the same time. For now, we assume a general view of objects because seeing, for example, just one side of a cube does not provide enough information on the extent of the whole object [10]. Even when assuming a general viewpoint, objects such as parallelepipeds or cylinders (objects with

surfaces where at least one principal curvature = 0) do not provide enough constraints for shape recovery with the inside-outside function alone. Parallelepipeds of different size satisfy equation (3) given range points on three or two adjacent faces. Among all those solutions we want to find the smallest superquadric that fits the given range points in the least squares sense. We have to find a function with a minimum corresponding to the smallest superquadric that fits a set of 3-D points *and* such that the function value for surface points is known before minimization. We define a new fitting function

$$R = \sqrt{a_1\, a_2\, a_3}\ (F - 1)\,, \tag{4}$$

which fulfills the first requirement with factor $(a_1\, a_2\, a_3)^{1/2}$ and the second requirement with factor $(F - 1)$. Due to the factor $(F - 1)$, function $R = 0$ for all points on the superquadric surface.

Now, we have to minimize the following expression

$$\min \sum_{i=1}^{N} [\, R\ (x_{W_1}, y_{W_1}, z_{W_1}; a_1\,, \ldots,\, a_{11})]^{\,2} \tag{5}$$

Since R is a nonlinear function of 11 parameters a_j, j=1 , . . . , 11, minimization must proceed iteratively. Given a trial set of values of model parameters Λ_k, we evaluate equation (4) for all N points and employ a procedure to improve the trial solution. The procedure is then repeated with a set of new trial values Λ_{k+1} until the sum of least squares (5) stops decreasing, or the changes are statistically meaningless. For most of test objects, 15 iterations were more then sufficient. We use the Levenberg-Marquardt method for nonlinear least squares minimization [11] since first derivatives $\partial R / \partial a_i$ for $i = 1\,, \ldots,\, 11$ can be computed analytically.

When testing the iterative model recovery method described in the previous section, we found that only very rough estimates of object's true position, orientation, and size suffice to assure convergence to a local minimum that corresponds to the actual shape. This is important since these parameters can be estimated only from the range points on the visible side of the object and hence the estimates cannot be very accurate to begin with. Initial values for both shape parameters, ε_1 and ε_2 can always be 1, which means that the initial model Λ_E is always an ellipsoid. Position in world coordinates is estimated by computing the center of gravity of all range points, and the orientation by computing the central moments with respect to the center of gravity. We orient the initial model so that the axis z of the object centered coordinate system lies along the longest side (axis of least inertia). This is because bending and tapering deformation normally affect objects along their longest side. Estimates for model's size are simply the extent of range points along the new coordinate axis. Figures 1, 2, 3 and 4 show examples of model recovery for each of the four proposed classes of mail; a box, a roll, a flat and an irregular postal piece (a banana in this case). The poor fit of the initial model in Figure 4 can be improved by using global deformations of superquadric models.

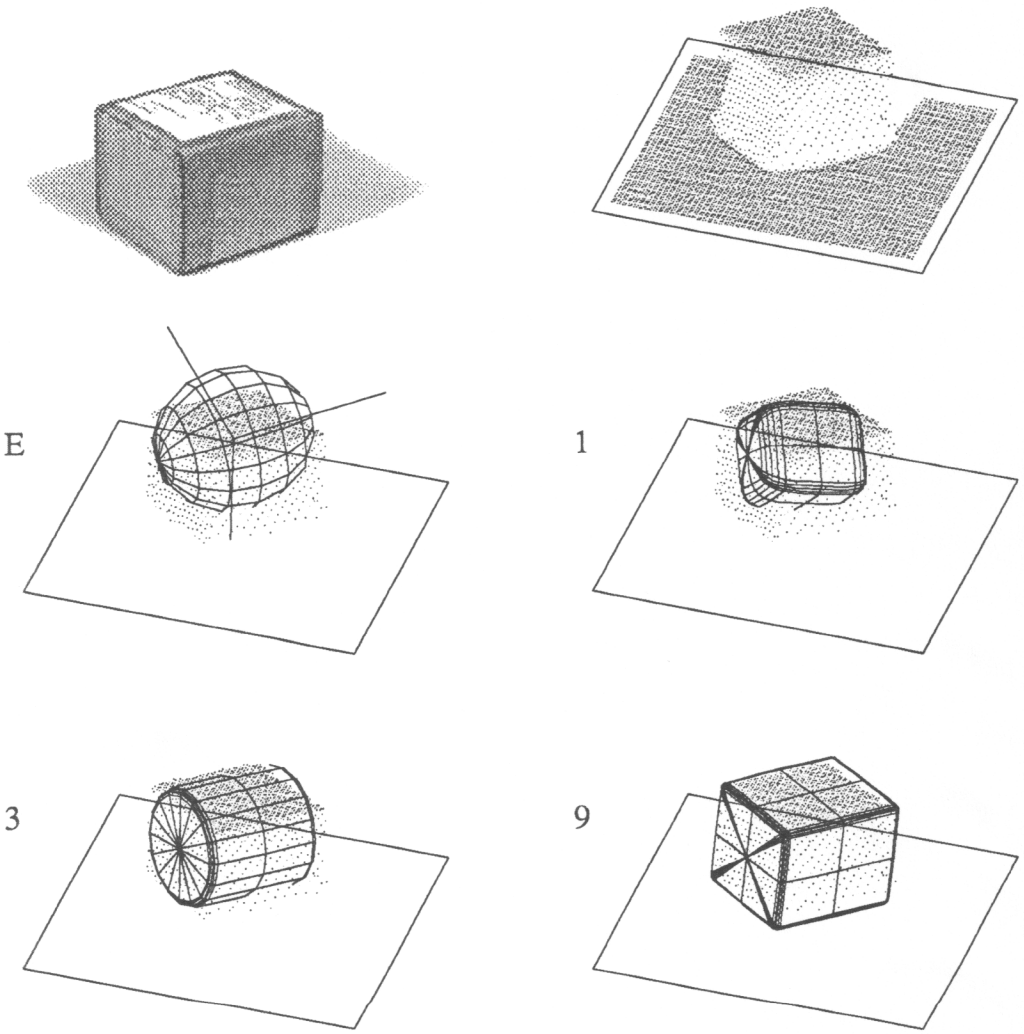

Figure 1. Shape recovery of a parallelepiped-like object - a box. On top are the intensity image and the corresponding range image. Below is the recovery sequence showing the initial estimate (E) and models after 1st, 3rd, and 9th iteration during which all 11 model parameters were adjusted. The above sequence only took about 20 seconds on a VAX 785 computer. The recovered parameters are: $a_1 = 54$ *mm*, $a_2 = 55$ *mm*, $a_3 = 63$ *mm*, $\varepsilon_1 = 0.1$, $\varepsilon_2 = 0.1$. Following the decision rules in Table 1, this object is classified as a *BOX* of *width* = 126 *mm*, *depth* = 108 *mm* and *height* = 110 *mm*.

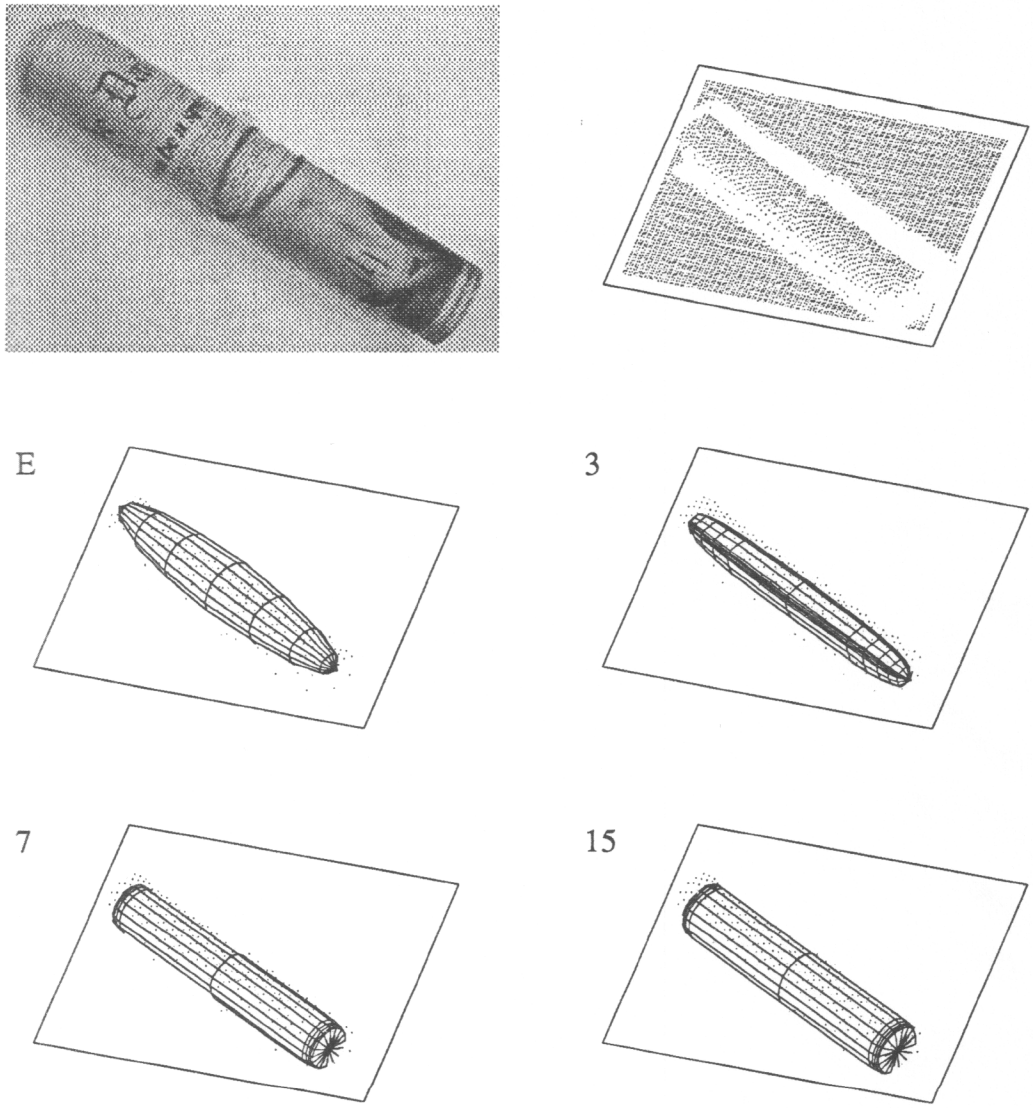

Figure 2. Shape recovery of a tube. On top are the intensity image and the corresponding range image. Below is the recovery sequence showing the initial estimate (E) and models after 3rd, 7th, and 15th iteration when all 11 model parameters were adjusted simultaneously. The recovered parameters are: $a_1 = 24\ mm$, $a_2 = 28\ mm$, $a_3 = 137\ mm$, $\varepsilon_1 = 0.1$, $\varepsilon_2 = 1.1$. Following the decision rules in Table 1, this object is classified as a *ROLL* of *lenght* = 274 *mm* and *diameter* = 52 *mm*.

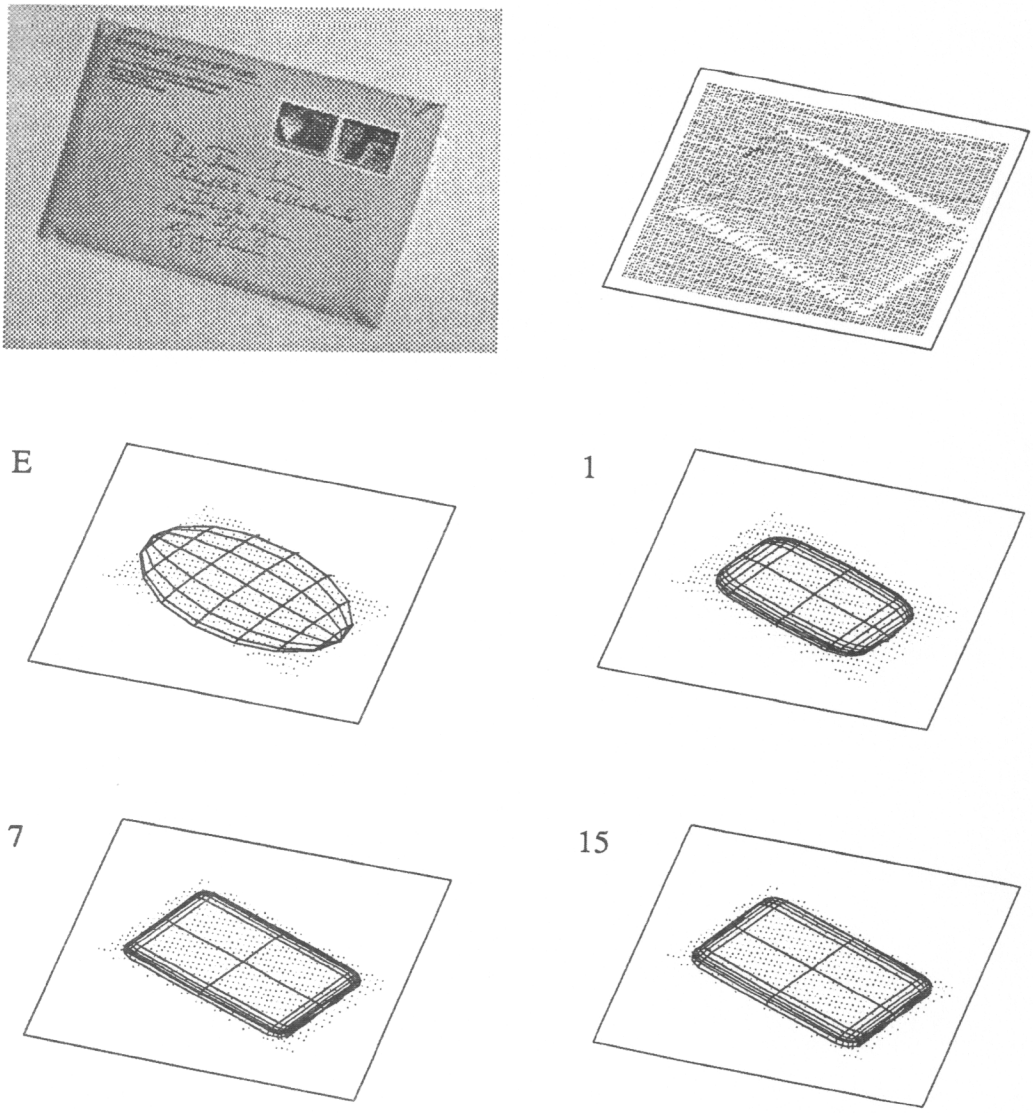

Figure 3. Shape recovery of a flat. On top are the intensity image and the corresponding range image. Below is the model recovery sequence showing the 1st, 7th, and 15th iteration when all 11 model parameters were adjusted simultaneously. The recovered parameters are: $a_1 = 5.5\ mm$, $a_2 = 63\ mm$, $a_3 = 98\ mm$, $\varepsilon_1 = 0.2$, $\varepsilon_2 = 0.3$. Following the decision rules in Table 1, this object is classified as a *FLAT* of $lenght = 196\ mm$, $width = 126\ mm$ and $thickness = 11\ mm$.

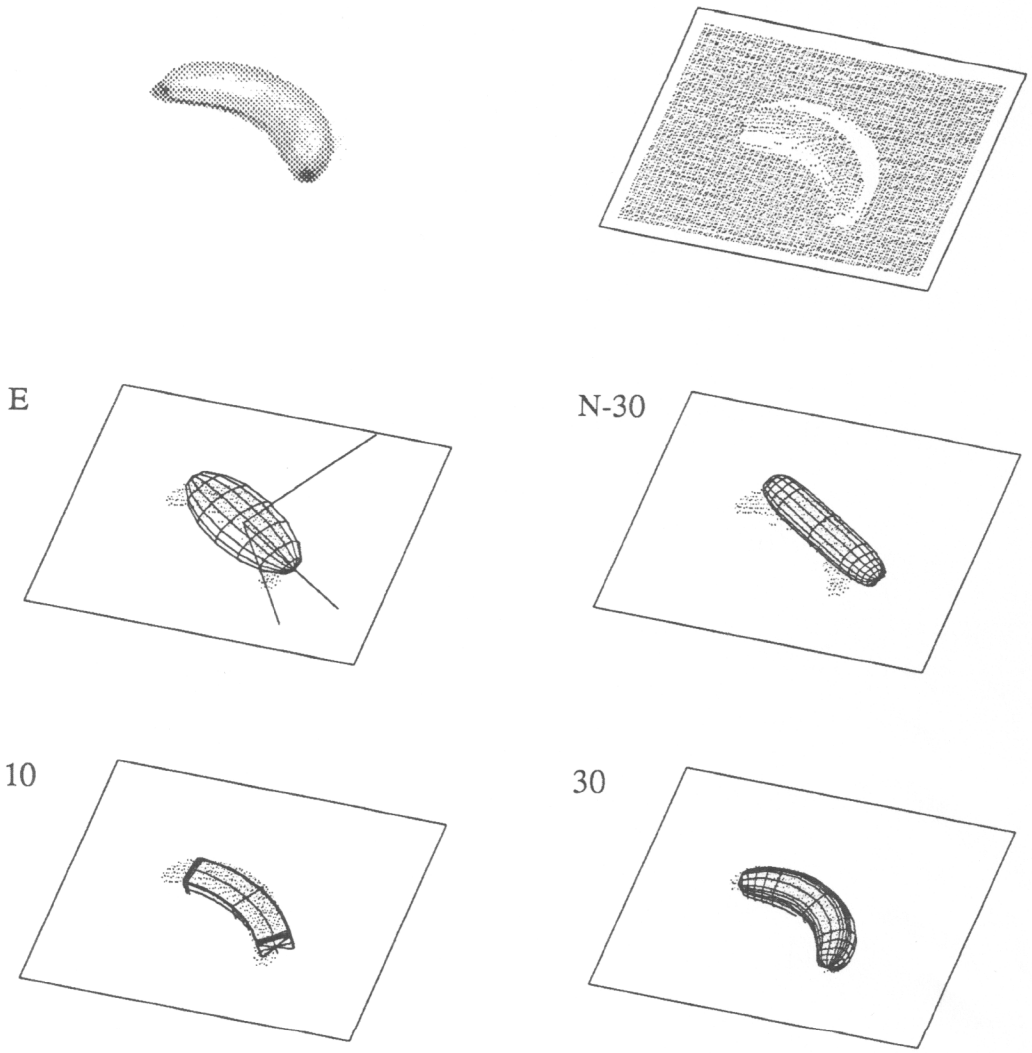

Figure 4. Shape recovery of a bent object - a banana.[1] On top are the intensity image and the corresponding range image. Below is the initial model estimate (*E*) and the recovered model after 30 iterations, without using any deformations. This fit (*N-30*) is quite poor - an indication that the object is an *irregular postal piece*. The model recovered using the built-in bending deformation achieves a better fit - shown are the 10th (*10*) and 30th iteration (*30*) of model recovery when a total of 13 model parameters were adjusted simultaneously. The recovered parameters are: $a_1 = 13\ mm$, $a_2 = 19\ mm$, $a_3 = 87\ mm$, $\varepsilon_1 = 0.6$, $\varepsilon_2 = 0.7$, *radius of the bend* $= 85\ mm$.

[1] A banana is certainly a highly unusual mail piece, but an article in the *Hartford Courant* on 10. October 1987 reported that a ripe yellow banana, with stamps and address on it, arrived by regular mail for a patient in a hospital in New Haven.

Deformed superquadrics can be recovered using the same technique as for the recovery of non-deformed superquadrics. The only difference is that some additional parameters describing deformations must be recovered also. Deformations such as simplified tapering, bending and twisting require just a few parameters [12]. A shape deformation is a function D which explicitly modifies the global coordinates of points in space

$$\mathbf{X} = D(\mathbf{x}) \tag{6}$$

where $\mathbf{x}$ are the points of the undeformed solid and $\mathbf{X}$ are the corresponding points after deformation. Both $\mathbf{x}$ and $\mathbf{X}$ are expressed in the object centered coordinate system. Any translation or rotation is performed after the deformation. A tapered and bent model can be described schematically as

$$Trans\ (Rot\ (Bend\ (Taper\ (\mathbf{x})))). \tag{7}$$

The corresponding inside-outside function of the deformable model that we implemented has 4 additional parameters; two tapering parameters (tangent of tapering angle in axis x and y: K_x, K_y), and two bending parameters (an angle to define the bending plane which goes through axis z - α, and the bending angle itself - β)

$$F(x, y, z) = F(X, Y, Z; a_1, \cdots, a_{11}, K_x, K_y, \alpha, \beta)\,. \tag{8}$$

The fitting function (equation 4) can be regarded as an energy function on the space of model parameters. Minimization methods can in general guarantee convergence only to a local minimum. It depends on the starting position in the parameter space (Λ_E) to which minimum will the minimization procedure converge. We have to assure that the minimization procedure does not get stuck in a shallow local minimum, but finds the deepest minimum. Shallow local minima are avoided as solutions during model recovery by adding Poisson distributed noise to the value of the fitting function of the accepted model before comparing it with the value of the fitting function of the model under consideration. This stochastic technique introduces ''jitter'' into the fitting procedure and resembles simulated annealing - see Figure 7.

We tested the consistency of the recovery method by taking range images of the same object in different positions and orientations. The recovered models compare favorably (Figure 5).

The most time consuming part in the described model recovery is the evaluation of the fitting function and of all of its partial derivatives for every input range point and during each iteration. Since the sum of least squares is a monotonically increasing function, it pays off to monitor the partial sum after each addition. As soon as the sum is larger than the sum of least squares of the accepted model, it makes no sense to continue. The model cannot be accepted. A substantial speed up can be achieved by subsampling the

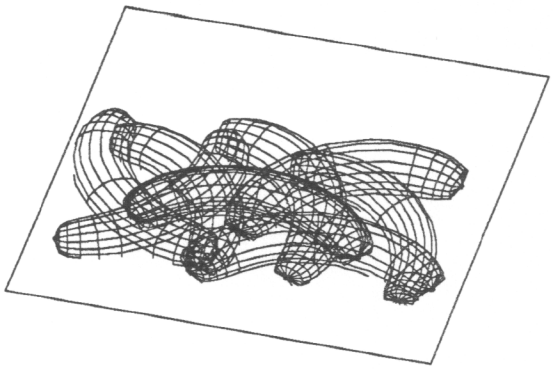

Figure 5. Recovered models of the same object (a banana) in 8 different positions and orientations. The recovered models are perceptually the same.

original range map. The models recovered from coarser range maps can still be a very good representation of the imaged object (Figure 6). During iterative model recovery, the fitting function typically drops very fast until it reaches a plateau. Further iterations gain no substantial improvements of fit (Figure 7). Fast and efficient computation can be done on a hierarchy of coarser grids. We implemented a multi-resolution model recovery scheme which starts on a very coarse range map. Once no improvement in fit is made, the minimization continues on a denser range map until the finest or the original range map is reached (Figure 7). Multi-resolution is faster because it takes less time for computation in each iteration. The number of iterations may not be smaller - it can get even larger because, during multi-resolution recovery, the model for a very sparse range map converges to a somewhat different set of parameters then required for representation of the actual object recorded on the finest level. Implementing the recovery procedure on a fine grained parallel architecture would be straightforward since the evaluation of the fitting function and its partial derivatives is independent for each range point. By assigning a processor to each range point, near real-time model recovery would be possible. A pyramid architecture would be an ideal choice for the multi-resolution scheme.

Recovery of models shown in this work, where the number of range points for each model is on the order of several hundred, takes about 20 seconds of CPU time on a VAX 785 computer. A detailed description of model recovery can be found in [5].

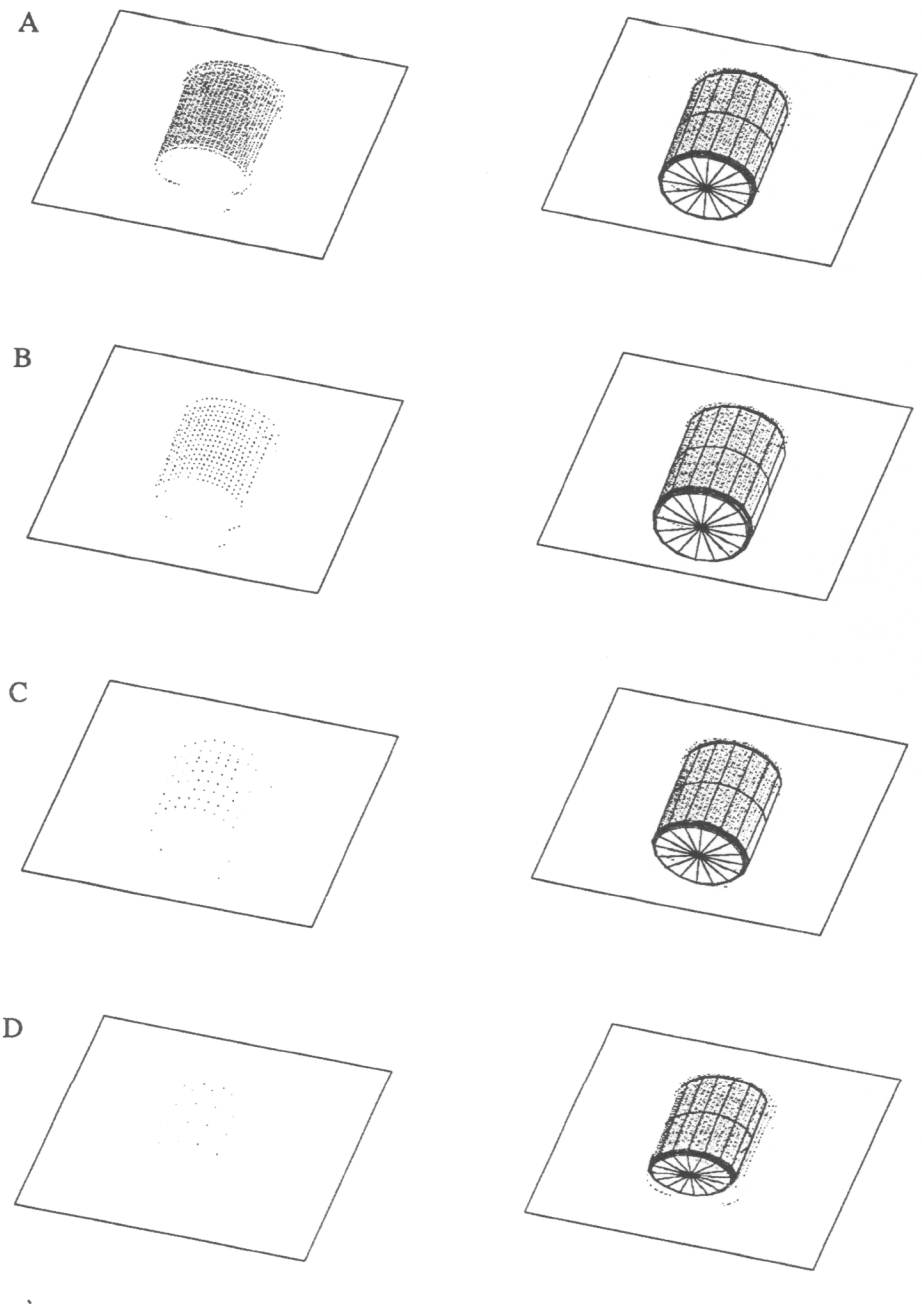

Figure 6. Influence of coarser range maps on the recovered models. On the left, from top down, are finer to coarser range maps, obtained by picking every 2nd (*B*), 4th (*C*) and 8th range point (*D*) in x and y axis of the original range map (*A*). On the right are the corresponding recovered models shown against the original range map.

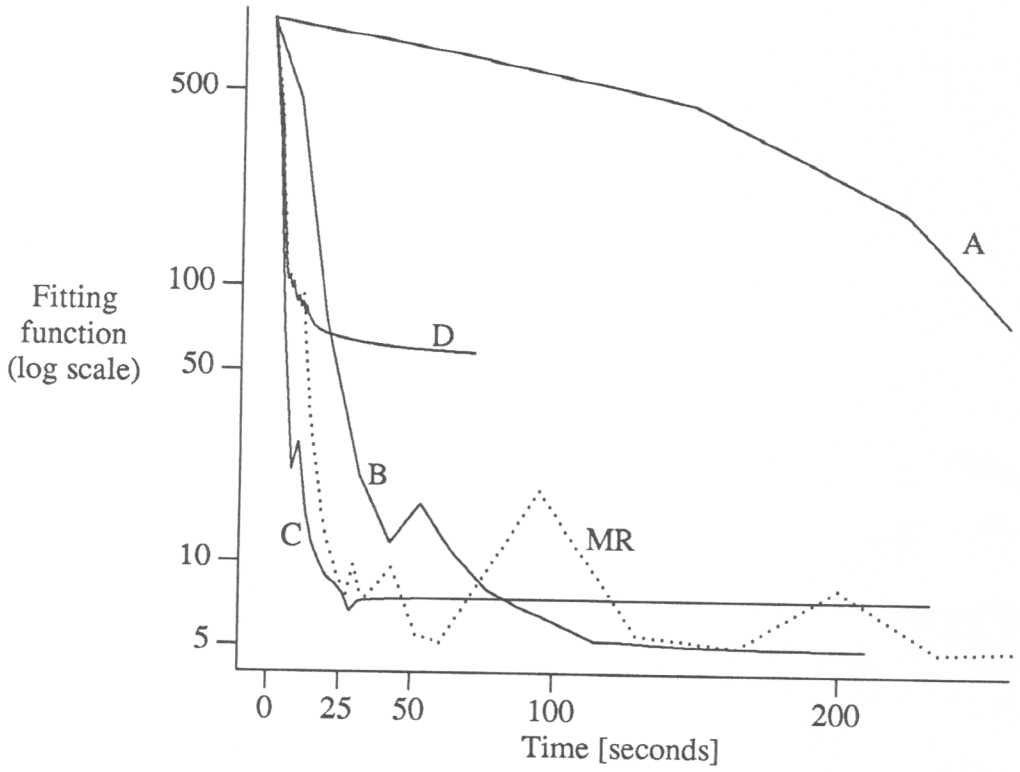

Figure 7. Fitting function as a function of CPU time on a VAX 785 computer during recovery of the four models (*A, B, C, D*) from Figure 6. The jaggedness of the function is due to the addition of Poisson noise which enables escaping from shallow local minima. When the fitting function reaches a plateau, the corresponding model cannot improve any more. The dotted line (*MR*) shows the fitting function for a multi-resolution fitting technique when model recovery starts on the coarsest map and switches to a finer map when the fitting function does not improve any more.

IV. CLASSIFICATION

The result of model recovery procedure are the position and orientation of models, as well as their size and shape parameters. The parameter space is continuous, but some sets of parameters correspond to easily identifiable geometric primitives such as parallelepipeds and cylinders. For those classes or categories, the within-category parameter differences look smaller than between-category parameter differences even when they are of the same size. By mapping symbols on the continuous parameter space it is possible to define distinctive classes of objects. For manual handling of mail pieces four classes of mail pieces evolved, reflecting natural breaks in the structure of mail shapes. The four classes are flats, boxes, tubes and irregular mail pieces as a class of all mail pieces that do not belong to any of the first three. We could define several different

classification schemes based on the recovered model parameters. Although the specification of the manipulation equipment for automatic mail handling must be taken into account, it makes sense to keep the existent classification, since it already reflects some sensible criteria for material handling. We can do even more. From the two shape parameters and size of the model, the actual radius of curvature on edges can be computed, to evaluate the sharpness or roundness of edges. Mail pieces that are normally lumped together into the class of irregular postal pieces can be better described with global deformations of tapering and bending. The least-squares minimization method for model recovery provides us with a measure of how good the model represents the actual object. This least-squares residuum is a measure of goodness of fit which plays a role in classification. The recovered model might be shaped as a parallelepiped but the goodness of fit can be very poor - indicating that the actual object is irregular (a film mailer, for example). The recovered model in this case is only a rough approximation fo the actual shape, but sufficient, for example, to grasp the object.

Based on the size of the model in all three axis (a_1, a_2, a_3), the two shape parameters ε_1 and ε_2, and goodness of fit, we designed the classification rules in Table 1.

input a_1, a_2, a_3, ε_1, ε_2, *residuum*,
K_{FLAT_t}, K_{FLAT_w}, K_{BOX}, K_{ROLL_dia}, K_{ROLL_len}, K_{RES}

if *residuum* $> K_{RES}$ **then** *mail piece is an IRREGULAR POSTAL PIECE*

else if [($a_1 < K_{FLAT\_t}$ **and** $a_2, a_3 > K_{FLAT\_w}$) **or**
($a_2 < K_{FLAT\_t}$ **and** $a_1, a_3 > K_{FLAT\_w}$)] **then** *mail piece is a FLAT*

else if [$a_1 > K_{BOX}$ **and** $a_2 > K_{BOX}$ **and** $a_3 > K_{BOX}$ **and**
$\varepsilon_1 < 0.5$ **and** $\varepsilon_2 < 0.5$] **then** *mail piece is a BOX*

else if [$a_1 > K_{ROLL\_dia}$ **and** $a_2 > K_{ROLL\_dia}$ **and** $a_3 > K_{ROLL\_len}$ **and**
$\varepsilon_1 < 0.5$ **and** $\varepsilon_2 > 0.5$] **then** *mail piece is a ROLL*

else *mail piece is an IRREGULAR POSTAL PIECE*

Table 1. Classification rules for mail pieces. According to the parameters and goodness of fit of recovered superquadric models, mail pieces are classified into four groups of mail: *BOXES, ROLLS, FLATS* and *IRREGULAR POSTAL PIECES*. A mail piece can be irregular either if the goodness of fit of the recovered model is not sufficient, as set by K_{RES}, or if its dimensions are not met by preset size limits. Constant K_{FLAT_t} determines the maximal thickness of a flat. Constant K_{FLAT_w} determines the minimal width and length of a flat. Constant K_{BOX} determines the minimal size of a box. Constant K_{ROLL_dia} sets the minimal radius of a roll and constant K_{ROLL_len} sets the minimal length for a roll.

V. DISCUSSION

The proposed shape vocabulary is intended for rough description of objects, suitable for shape classification of mail pieces. Objects whose occluded side is not symmetrical to the visible side might not get represented adequately. Although deformations are often sufficient, they do not cover all possible cases. A larger number of different deformations could be used, but that would require a larger number of parameters. The model that we use seems to be adequate for grasping and handling of objects.

Nonuniform range data density and a large number of singular views in range images was another problem that we faced. Nonuniform range point density causes that parts with higher density have more influence on the shape of the recovered model then parts with lower density. However, the model recovery method is quite robust in this regard - note that no range data is available from occluded parts to begin with. In a singular view, on the other hand, when only one face of a cube is seen, a very thin parallelepiped which fits to that face would be recovered. Images taken with a passive range imager, which uses triangulation, have more singular views than normally associated with intensity images. The larger the distance (angle) between the source of illumination and the camera of the range imager, the better the accuracy, but the more singular views, since range points must be illuminated *and* seen by the camera at the same time. Singular views can be resolved by taking into account the structure of the surrounding scene. Objects normally rest on some support, they can touch and they do normally not penetrate each other. Currently we solve the problem of singular views by projecting the visible points to the support surface and use them together with the rest of points for fitting. This resolves the problem for singular views but distorts other objects, like a cylinder laying on its side. The problem can be resolved by recovering a model for both cases, fitting first a model only to the visible points, and then to the visible points and their projection onto the supporting surface. If the goodness of fit is about the same in both cases we select the model with the larger volume. Otherwise the model with the better goodness of fit is selected. Witkin, Fleischer and Barr [13] developed an elegant method for describing geometric relations between part or objects in terms of energy constraints. When using this paradigm, a sum of energy terms would have to be minimized, one of them being the fitting function, while other terms would constrain geometrical relations.

In this paper we concentrated only on shape recovery of single mail pieces. When several possibly overlapping mail pieces are present in the scene, the scene must be segmented - each mail piece should be represented with a single model. Segmentation, however, depends on the shape of individual parts. For recovery of parts again, one should know which range points belong together. Because of this inter-depedence, we believe that segmentation and shape recovery of individual parts should be done simultaneously. By allowing a variable number of range points in a model, a model can actively search for a better fit, resulting in a subdivision of the scene into pieces, each represented with with a single superquadric. More about segmentation with deformable part models can

be found in [5].

ACKNOWLEDGEMENTS

This research was supported by the U.S. Postal Service contract 104230-87-H-0001/M-0195. We thank Gus Tsikos, K. Wohn and Alok Gupta for help in obtaining range images and discussing classification schemes.

REFERENCES

[1] R. C. Bolles and P. Horaud, "3DPO: A Three-Dimensional Part Orientation System." *International Journal of Robotics Research*, vol. 5, no. 3, pp. 3-26, 1986.

[2] D. Marr, *Vision*. San Francisco: Freeman, 1982.

[3] F. Solina and R. Bajcsy, "Modeling of Mail Pieces with Superquadrics," in *Proceedings USPS Advanced Technology Conference*, Washington, DC, 1986, pp. 472-481.

[4] F. Solina and R. Bajcsy, "Range Image Interpretation of Mail Pieces with Superquadrics," in *Proceedings AAAI-87*, Seattle, 1987, pp. 733-737.

[5] F. Solina, "Shape recovery and segmentation with deformable part models." Ph.D. dissertation, University of Pennsylvania, Philadelphia, 1987.

[6] G. Tsikos, "Segmentation of 3-D scenes using multi-modal interaction between machine vision and programmable mechanical scene manipulation." Ph.D. dissertation, University of Pennsylvania, Philadelphia, 1987.

[7] A. H. Barr, "Superquadrics and angle-preserving transformations." *IEEE Computer Graphics and Applications*, vol. 1, pp. 11-23, 1981.

[8] A. P. Pentland, "Perceptual Organization and the Representation of Natural Form." *Artificial Intelligence*, vol. 28, no. 3, pp. 293-331, 1986.

[9] R. Paul, *Robot Manipulators*. Cambridge, MA: MIT Press, 1981.

[10] J. Koenderink and A. van Doorn, "The internal representation of solid shape with respect to vision." *Biological Cybernetics*, vol. 32, pp. 211-216, 1979.

[11] W. H. Press, B. P. Flannery, S. A. Teukolsky, and W. T. Vettering, *Numerical Recipes*. Cambridge: Cambridge University Press, 1986.

[12] A. H. Barr, "Global and local deformations of solid primitives." *Computer Graphics*, vol. 18, no. 3, pp. 21-30, 1984.

[13] A. P. Witkin, K. Fleischer, and A. Barr, "Energy constraints on parameterized models," in *Proceedings SIGGRAPH-87*, Anaheim, CA, July 1987.